

Preparation of an Ideal Thin Mercury Film Electrode and Its Electrochemical Property

Zenko YOSHIDA

Chemistry Division, Japan Atomic Energy Research Institute, Tokai, Ibaraki 319-11

(Received May 6, 1980)

In order to get an ideal thin mercury film electrode, the structure of mercury film electrodeposited on foreign metals was investigated with the aid of the thermal-evaporation behavior of mercury and correlated to the electrode properties of the mercury-deposited surfaces. A mercury layer deposited on gold, copper, nickel, or platinum consists of stable mercury compounds with the base metal at their interface and a uniform metallic mercury layer on them. The hydrogen(H)-overpotential at the mercury-coated surface increases with the increase in the amount of mercury deposited. Mercury on molybdenum or stainless steel forms island-like metallic mercury droplets by electrodeposition. The H-overpotential at the surface is identical with that at molybdenum or stainless steel without mercury. Mercury deposited on lead or zinc easily forms a stable amalgam with the base metal, and no metallic mercury is present. The H-overpotential at the surface is slightly less than that at a base metal without mercury. A nickel-based thin mercury film electrode is recommended for such electroanalytical uses as anodic stripping voltammetry.

Thin mercury film electrodes (TMFE) are widely used¹⁻⁶⁾ in such electroanalytical fields as stripping analysis. Platinum and silver are usually used as base metals of such TMFE. It has been well known^{1,4)} that the hydrogen(H)-overpotential at the TMFE is less than that at pure mercury, even when a fairly large amount of mercury is deposited, and that the H-overpotential decreases with the standing time. These disadvantages of the TMFE restrict the electrochemical and analytical use of the TMFE. Generally, the reason for the lowering of the H-overpotential has been empirically understood^{1,4)} as the diffusion of base metal atoms into the mercury layer or the droplet formation of deposited mercury. However, few reports have discussed the H-overpotential at the mercury-coated electrode theoretically and systematically.

Regarding with the hydrogen-evolution reaction or other electrode properties at thin metal film electrodes, combinations of deposited metals and base metals are divided into two groups.⁷⁾ In one group, the monolayer metal deposited shows an electrode property identical with that at the pure metal to be deposited,⁸⁻¹⁰⁾ while in the other the electrode property at the thin metal film electrode is different from that at the pure metal, even when the amount of metal deposited is fairly large.^{7,11)} As a typical example of the latter, the mercury-coated platinum electrode was investigated in the preceding report.⁷⁾ The cause of the gradual change in electrode properties with the increase in the amount of mercury was explained by the development of the stable platinum-mercury intermetallic compounds, which affect the electrode property of the surface of mercury deposited. Moreover the decrease in the H-overpotential with the standing time was attributed to the formation of PtHg₄.

From the analytical point of view, a stable indicator electrode with a large H-overpotential is required. Mercury is indispensable because of its large H-overpotential. On the other hand, a suitable base metal for the TMFE should make the stable mercury layer both mechanically and chemically and should not lower the H-overpotential of mercury.

In the present report, the structure of the mercury

layer deposited and the hydrogen-evolution reaction at the deposited mercury surface are studied employing gold, copper, nickel, molybdenum, lead, zinc, and stainless steel as base metals. On the basis of these results, a criterion for selecting the most preferable metal as the base metal of the TMFE is suggested.

Experimental

The metals used were of purities more than 99.9%. Mercury (II) and supporting electrolyte solutions were prepared using specially purified water as has been reported previously.⁷⁾ The electrolytic measurement and determination of mercury vapor by flameless atomic absorption spectrophotometry (AAS) were carried out by means of the apparatus described in the previous paper.⁷⁾ The electrolytic measurements were carried out at $25 \pm 0.5^\circ\text{C}$, and the potentials were referred to a saturated calomel electrode (SCE) unless otherwise mentioned. The surface area of the electrode was 1.13 cm^2 .

Pretreatments of the Metals.¹²⁾ The gold, copper, nickel, molybdenum, lead, zinc, and stainless steel used as base metals were electropolished anodically by using a stainless steel cathode at applied potentials of 6 V in a cyanide bath,¹³⁾ at 5 V in 60% phosphoric acid in water, at 5 V in 60% sulfuric acid in water, at 5 V in 12.5% sulfuric acid in methanol, at 6 V in 60% nitric acid in methanol, at 2.5 V in 20% nitric acid in methanol, and at 8 V in 64% phosphoric acid + 15% sulfuric acid in water, respectively. Then the polished metals were washed with water.

Deposition of Mercury. Mercury was electrodeposited on metals, except on copper, by controlled-potential electrolysis for 15 min in a deaerated electrolyte solution which contained various concentrations of mercury (II), $1 \times 10^{-1}\text{ M}$ ($1\text{ M} = 1\text{ mol dm}^{-3}$) in potassium perchlorate, and $1 \times 10^{-3}\text{ M}$ in perchloric acid. The electrodeposition potentials of mercury on gold, nickel, molybdenum, lead, zinc, and stainless steel were at +0.20, -0.45, -0.10, -0.50, -1.30, and 0.0 V, respectively. Mercury was deposited on copper spontaneously when the copper plate was dipped in a solution containing mercury (II).

H-overpotential Measurements. The hydrogen-reduction peak potential, E_p , in a cyclic voltammogram which was obtained in $1 \times 10^{-1}\text{ M}$ potassium perchlorate and $1 \times 10^{-3}\text{ M}$ perchloric acid at a potential scanning rate of 2 mV s^{-1} was employed for convenience in studying the H-overpotential.⁷⁾ The cathodic potential scan was started at potentials about

50 mV more negative than the dissolution potential of the electrode. The galvanostatic measurements were carried out by the procedures described previously.⁷⁾

Thermal Evaporation of Mercury (*T*-Hg curve). In order to ascertain the structure of the mercury layer deposited, the thermal-evaporation behavior of mercury was investigated by means of the procedure and apparatus reported previously.^{7,13)}

Results

Mercury-coated Gold, Copper, or Nickel. *Structure of Mercury Deposited:* A mercury-coated electrode was heated in an argon stream (2 l min^{-1}) at a raising rate of temperature of $20^\circ\text{C min}^{-1}$, and the evaporated mercury was detected by means of flameless AAS (*T*-Hg curve).¹³⁾ With the increase in the amount of mercury, one to four peaks were observed.

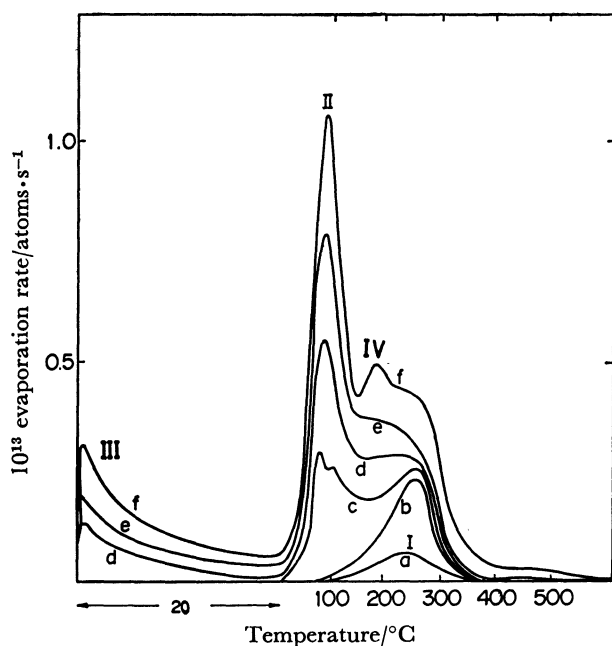


Fig. 1. *T*-Hg curves of mercury deposited on gold. Amounts of mercury deposited ($\mu\text{g cm}^{-2}$): (a) 0.07, (b) 0.20, (c) 0.50, (d) 0.97, (e) 1.28, (f) 2.32.

The *T*-Hg curves of mercury, $0.07\text{--}2.3 \mu\text{g cm}^{-2}$, deposited on gold are illustrated in Fig. 1. Peaks I, II, III, and IV are observed at 243, 100, 20, and 160°C , respectively. These *T*-Hg curves are analogous to those of mercury deposited on platinum.⁷⁾ By comparing them with the results of the detailed investigations of mercury on platinum⁷⁾ or gold¹³⁾ in the previous papers, Peaks I, II, III, and IV in Fig. 1 are identified as the mercury evaporations from a stable first mercury layer, metallic mercury, adatom mercury, and alloy between gold and mercury, respectively. With a small amount of mercury (less than $0.20 \mu\text{g cm}^{-2}$), only Peak I is observed, and this peak is saturated at $0.20 \mu\text{g cm}^{-2}$. In the previous study,⁷⁾ the structure of the first mercury layer on platinum was confirmed to be Pt_2Hg . Assuming that each mercury atom deposited is combined with one platinum or gold atom of the electrode surface, with a roughness factor of unity, the amount of mercury

which makes the complete monolayer should be about $0.5 \mu\text{g cm}^{-2}$, because the lattice constants of platinum or gold are nearly equal to 4 \AA . In view of the saturated amount of the first mercury layer on gold ($0.20 \mu\text{g cm}^{-2}$), and the generally accepted structure of stable mercury-gold intermetallic compounds,¹⁴⁾ the first mercury layer on gold is considered to be Au_xHg , where x is 2 or 3.

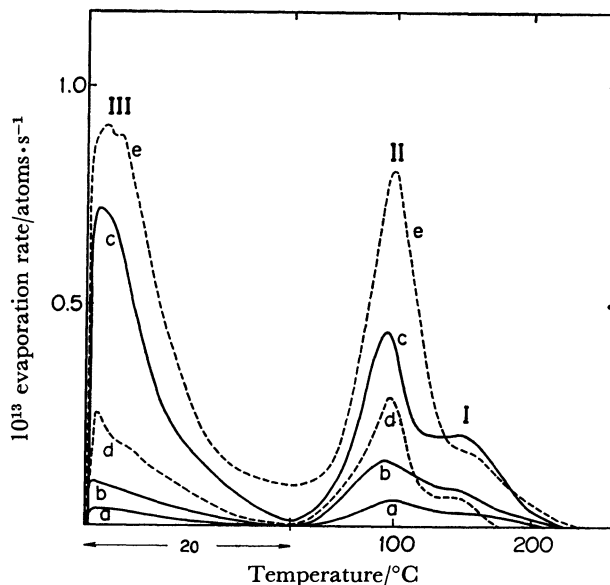


Fig. 2. *T*-Hg curves of mercury deposited on copper and nickel.

Amounts of mercury deposited ($\mu\text{g cm}^{-2}$): (a) 0.06, (b) 0.16, (c) 0.64, (d) 0.25, (e) 0.95. Based metal: (a)–(c) copper, (d), (e) nickel.

The mercury layer deposited on copper or nickel shows a different *T*-Hg behavior from those on platinum and gold, as is shown in Fig. 2. Even when less than $0.20 \mu\text{g cm}^{-2}$ of mercury is deposited, three peaks are observed in the *T*-Hg curves, i.e., Peak I at about 160°C , Peak II at 100°C , and Peak III at about 20°C . With the increase in mercury, these peaks develop and Peak I is not saturated. The mercury evaporates from the stable layer at a lower temperature (Peak I at 160°C) than that of mercury on platinum or gold, indicating that the interaction between mercury and copper or nickel is less than that between mercury and platinum or gold. The idea of a small interaction is also supported by the large adatom layer on copper or nickel, shown in Fig. 2, because a large amount of the adatom layer was formed on the glassy carbon (GC) electrode,¹⁵⁾ which has very weak interaction with mercury. The absence of any preferential saturation of the stable mercury layer on copper or nickel can also be explained by the small interaction with mercury.

The large amount of mercury ($100\text{--}250 \mu\text{g cm}^{-2}$) deposited on gold, copper, or nickel shows the *T*-Hg curves shown in Fig. 3. The *T*-Hg curves of mercury deposited on platinum⁷⁾ or GC¹⁵⁾ previously investigated are also illustrated in this figure. The mercury deposited on GC is purely metallic and is unstable from the mechanical point of view, for no stable mercury layer

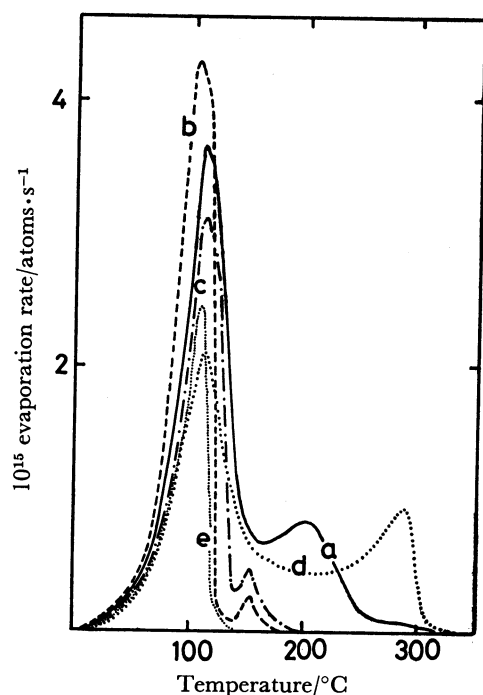


Fig. 3. T-Hg curves of mercury deposited on gold, copper, nickel, platinum, and glassy carbon. Amounts of mercury deposited ($\mu\text{g cm}^{-2}$): (a) 230, (b) 172, (c) 138, (d) 190, (e) 97. Based metal: (a) gold, (b) copper, (c) nickel, (d) platinum, (e) glassy carbon.

is formed at the GC-mercury interface. The mercury layer deposited on platinum or gold consists of the stable mercury and metallic mercury layer, and the stable mercury occupies quite a large portion of the total deposited mercury, while a small amount of the stable mercury is formed in the mercury layer deposited on copper or nickel. The mercury layer on copper or nickel is mechanically stable because of the interaction between mercury and the base-metal surfaces, though the

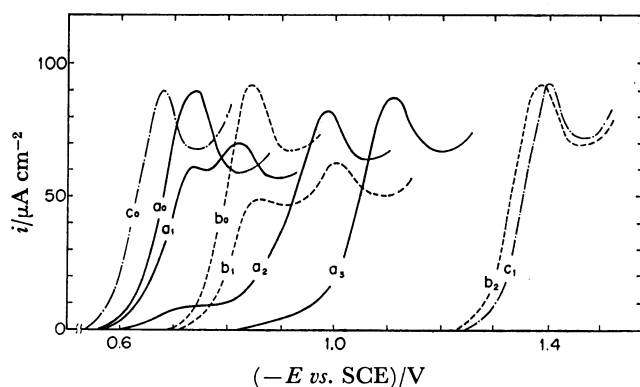


Fig. 4. Cyclic voltammograms for hydrogen evolution at gold, copper, and nickel electrodes with and without mercury. Electrolyte: 1×10^{-1} M potassium perchlorate and 1×10^{-3} M perchloric acid. Rate of potential scanning: 2 mV s^{-1} . Based metal: (a) gold, (b) copper, (c) nickel. Amounts of mercury deposited ($\mu\text{g cm}^{-2}$): (a_0) 0, (a_1) 0.40, (a_2) 0.85, (a_3) more than 1.0, (b_0) 0, (b_1) 1.1, (b_2) more than 80, (c_0) 0, (c_1) more than 100.

interaction is rather small.

Hydrogen-evolution Reaction at Mercury-coated Gold, Copper, or Nickel.

The cathodic parts of cyclic voltammograms for hydrogen evolution in an electrolyte solution containing 1×10^{-1} M in potassium perchlorate and 1×10^{-3} M in perchloric acid, obtained at the gold, copper, or nickel electrode with and without mercury, are shown in Fig. 4. The cyclic voltammograms in the second potential scan are adopted in order to determine the H-overpotential at mercury-coated metals for the same reason as in the previous paper.⁷⁾ Two waves are frequently observed in voltammograms when the amount of mercury is small. The first peak corresponds to the hydrogen evolution at the base-metal surface which is not covered with mercury. The peak potential of this wave is identical with that at a base metal without mercury, and the peak current of this wave decreases with the increase in mercury. The second peak potential is employed as the H-overpotential at a mercury-coated electrode.

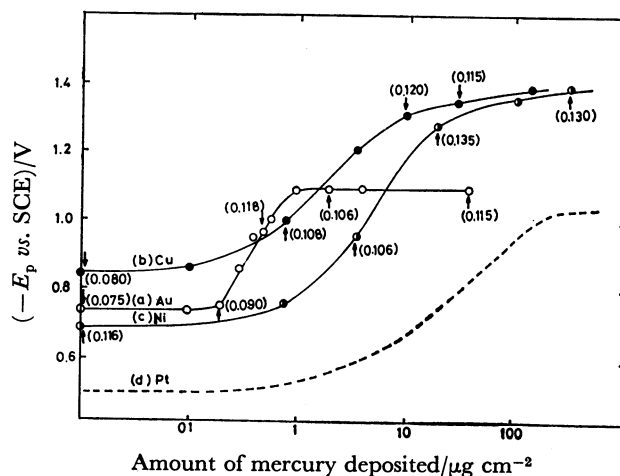


Fig. 5. Hydrogen overpotential, E_p , and Tafel slope, b , at mercury-coated gold, copper, and nickel with various amounts of mercury. Based metal: (a) gold, (b) copper, (c) nickel, and (d) platinum (-----).

The relation between the amount of mercury deposited and the second peak potential, E_p , observed is illustrated in Fig. 5. The value in parentheses indicates the Tafel slope, b ⁷⁾ (in V), for the hydrogen-evolution reaction at the electrode which corresponds to the plot indicated with an arrow. When two waves are observed in a cyclic voltammogram, the Tafel slope for the second wave is employed. The dashed curve (d) shows the relation for mercury deposited on platinum, which was reported in the previous paper.⁷⁾ With the increase in the amount of mercury deposited, the b slope increases and E_p shifts to a more negative value. As has been described in the preceding section, the coverage of the surface of a gold or platinum electrode is complete with the deposition of a monolayer amount of mercury because of the large interaction between gold or platinum and mercury. E_p does not change from that at mercury-free gold or platinum when less than a monolayer amount

of mercury is deposited. With a larger amount of mercury than the monolayer, the coverage with the mercury deposited is considered not to be uniform because of the small interaction between the first mercury layer and the subsequent mercury layer to be deposited. Moreover, it is obvious from the T -Hg curve that compounds are formed between a base metal and mercury. On the other hand, the preferential monolayer formation is not observed when mercury is deposited on copper or nickel, because the interaction between these base metals and mercury is small. Also, the coverage of the surface increases slowly with the increase in the amount of mercury. Therefore, the gradual change in E_p with the increase in the amount of mercury, as shown in Fig. 5, is attributable both to the change in the coverage of the electrode surface and to the formation of the stable compounds.

When more than 1, 80, and 100 $\mu\text{g cm}^{-2}$ of mercury are deposited on gold, copper, and nickel, the E_p values show limiting values, E_p^1 , at -1.10 , -1.38 , and -1.40 V, respectively. These E_p^1 values are more positive than that at the HMDE.

Stability of Mercury Layer Deposited on Gold, Copper, or Nickel.

When the mercury ($200 \mu\text{g cm}^{-2}$)-coated copper was allowed to stand at 25°C for 70 h in a deaerated supporting-electrolyte solution, Peak II at 110°C in the T -Hg curve (b) in Fig. 3 decreased to one-half of the initial peak height; instead, a peak at 164°C and an additional peak at 175°C develop. With the same standing time (70 h), E_p for hydrogen evolution shifted from -1.38 to -1.10 V. In view of the results of the previous study of the mercury-coated platinum,⁷⁾ the effect of the standing time on the T -Hg curve and H-overpotential may be attributed to the structural change in the deposited mercury layer due to the alloy formation of mercury with copper which has diffused into the mercury layer. In this connection, the peak height at 110°C in the T -Hg curve for the mercury ($200 \mu\text{g cm}^{-2}$)-coated platinum decreased to one-half within the standing time of only 3 h, as has been reported previously,⁷⁾ and E_p shifted from -1.05 to -0.95 V during the standing.

The mercury ($200 \mu\text{g cm}^{-2}$)-coated gold and nickel are chemically stable, and no change in the T -Hg curve or H-overpotential is observed with a standing time of up to 70 h.

Mercury-coated Molybdenum or Stainless Steel. Only the peak at 110°C was observed in the T -Hg curves for mercury (0 – $500 \mu\text{g cm}^{-2}$) deposited on these metals. No peak at a higher temperature in the T -Hg curve was observed, even when the amount of mercury was increased up to 2 – 3 mg cm^{-2} and when the mercury-coated electrode was allowed to stand for 70 h. By considering the analogous T -Hg curve of mercury deposited on the GC electrode,¹⁰⁾ it is clear that the chemical interaction between mercury and molybdenum or stainless steel is negligibly small. In addition, the amount of mercury deposited on these metals decreased with the standing time.

Cyclic voltammograms at mercury (0 – $500 \mu\text{g cm}^{-2}$)-coated molybdenum or stainless steel were identical with those at mercury-free molybdenum or stainless

steel; i.e., the E_p values were -0.78 or -0.81 V, respectively.

These results indicate that mercury deposited on these metals forms an island-like deposit instead of a stable mercury layer and that the coverage of the surface of these metals by mercury is incomplete.

Mercury-coated Lead or Zinc. Mercury deposited on lead or zinc formed stable compounds with the base metal and no metallic mercury layer existed at the electrode surface, even when the amount of mercury was 1 mg cm^{-2} ; this is apparent in the T -Hg curves in Fig. 6.

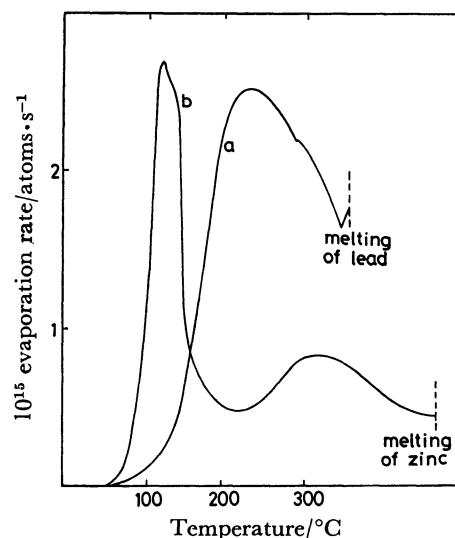


Fig. 6. T -Hg curves of mercury deposited on lead and zinc.

Amounts of mercury deposited: more than 1 mg cm^{-2} .
Based metal: (a) lead, (b) zinc.

The hydrogen-evolution potentials, E_p , at a large amount of mercury (about 1 mg cm^{-2})-coated lead or zinc were at -1.43 or -1.32 V, about 100 mV more positive than those at mercury-free lead (at -1.50 V) or zinc (at -1.43 V).

Discussion

Considering the structure of the mercury layer deposited on metals and the hydrogen-evolution reactions at their surfaces described in the Results, base metals can be classified into three groups.

The metals in Group I have fairly large interactions with mercury, and stable mercury layers are formed at the mercury-base metal interfaces. With more than $0.3 \mu\text{g cm}^{-2}$ of mercury, a metallic mercury surface appears. The H-overpotentials at mercury-coated surfaces increase with the increase in mercury until the limiting potentials, E_p^1 , are reached.

The metals in Group II have negligibly small interactions with mercury, and the mercury deposited on these metals forms island-like metallic mercury deposits. The mercury is mechanically unstable. The H-overpotentials at the surfaces on which mercury is deposited are identical with those at mercury-free surfaces.

The metals in Group III form very stable amalgams with mercury, and metallic mercury does not coexist, even when 1 mg cm^{-2} of mercury is deposited. The H-overpotentials at their surfaces are slightly less than those at mercury-free surfaces.

Gold, copper, nickel, and platinum belong to Group I, molybdenum and stainless steel, (and GC) to Group II, and lead and zinc, to Group III.

An ideal thin mercury film electrode (TMFE) should be stable both mechanically and chemically, and it should have a large H-overpotential. In view of these requirements for the TMFE, the metals in Group I are most suitable as the base metals.

The strength of the interaction between mercury and the base metal determines the mechanical stability of mercury film; this strength is semi-quantitatively given by the peak-temperature difference between the evaporation of mercury from the stable mercury layer and the metallic mercury layer, ΔT , in the T -Hg curve. A large ΔT value certifies a stable mercury layer. On the other hand, too large ΔT value reduces the chemical stability and decreases the H-overpotential because of the structural change in the mercury layer during standing (alloy formation). For example, the H-overpotential at the mercury-coated platinum, the ΔT value of which was 190°C , was remarkably changed with standing.⁷⁾ Among the metals studied in the present work, the best base metal for the TMFE was nickel, the ΔT value of which was about 50°C .

Although ΔT was conventionally used to ascertain the qualitative evaporation behavior of mercury, the activation free energy of thermal evaporation, ΔG^* , was also investigated for a more quantitative treatment. The activation free energy was determined using a procedure similar to that described previously.¹³⁾ The differences between the ΔG^* value for the evaporation of the stable mercury and that for metallic mercury, $\Delta(\Delta G^*)$, here obtained were 0.98, 0.42, 0.16, and 0.16 eV for mercury deposited on platinum, gold, copper, and nickel, respectively.

The interaction between the deposited metal and the base metal has been electrochemically recognized as an underpotential¹⁶⁾ for the metal deposition. Kolb *et al.*¹⁷⁾ expressed the underpotential shift, ΔU , correlating to the work function difference between the deposited metal and the base metal, $\Delta\phi$, by using an empirical equation (1):

$$\Delta U = 0.5 \Delta\phi/e, \quad (1)$$

where ΔU was the difference in peak potentials between the anodic oxidation of the stable layer and the bulk layer, as determined from an anodic stripping voltammogram (ASV). Employing the work function values of 5.40 and 4.50 eV for platinum and mercury reported in Ref. 19, ΔU is calculated to be 0.45 V for mercury deposition on platinum by using Eq. 1. On the other hand, if the rate-determining step in both the thermal evaporation and anodic oxidation reactions is assumed to be the same and is a breaking of the metal bond, producing an atom to be evaporated or oxidized, ΔU can be expressed by using ΔG^* , as in Eq. 2:

$$\Delta U = \Delta(\Delta G^*)/ne, \quad (2)$$

where n is the number of electrons involved in the anodic oxidation reaction. By using the experimentally obtained value as $\Delta(\Delta G^*)$, 0.98 eV for mercury on platinum, and Eq. 2, ΔU is found to be 0.49 V. The underpotential, ΔU , for mercury deposition on platinum has been reported as 0.47 V by Bruckenstein *et al.*¹⁸⁾ and Kolb *et al.*¹⁷⁾ using the ASV curve. In the previous report,⁷⁾ ΔU was determined to be 0.45 V from the relation between the electrolysis potential and the amount of mercury deposited (E -Hg plot). For mercury deposition on gold, ΔU was determined as 0.20 V using the E -Hg plot, as has been reported previously.¹⁸⁾ ΔU is calculated as 0.14 V using Eq. 1 or as 0.21 V using Eq. 2. Here, as a work-function value of gold, the value of 4.78 eV which was recommended by Trasatti¹⁹⁾ is employed, although the reported values are distributed from 4.78 to 5.32 eV.²⁰⁾ The good agreement between the ΔU values calculated from both Eqs. 1 and 2 and the experimental values indicates that ΔU can be correlated to $\Delta(\Delta G^*)$ and $\Delta\phi$, and that the relation between $\Delta\phi$ and $\Delta(\Delta G^*)$ can be expressed by Eq. 3:

$$\Delta(\Delta G^*) = 0.5 n \Delta\phi. \quad (3)$$

Although ΔU cannot be experimentally determined for mercury deposition on copper or nickel using the electrochemical method because of the anodic dissolution of the electrode, ΔU can be predicted from the T -Hg curve by using Eq. 2 to be 0.08 V for the mercury deposition on these metals. The ΔU values are also calculated using Eq. 1 to be 0.03–0.10 and 0.12 V by using the work-function values of copper, 4.55–4.70,^{19,21)} and nickel, 4.73 eV,¹⁹⁾ respectively.

Because interaction between deposited and base metals is a function of $\Delta\phi$, as has been mentioned above, the general criterion for selecting a suitable TMFE and other metal-film electrodes can be expressed using the work function, which is a general physicochemical parameter and which has been determined for a number of metals. For the ideal TMFE, $\Delta\phi$ should be large enough to form a stable mercury layer with respect to the mechanical stability and should be small with respect to the chemical stability and E_p^\dagger . The reason has not yet been explained, but E_p^\dagger is more negative with a small value of $\Delta\phi$. $\Delta\phi$ and E_p^\dagger for the mercury-coated platinum, gold, copper, and nickel are 0.90, 0.28, 0.05–0.20, and 0.23 eV, and -1.05 , -1.10 , -1.38 , and -1.40 V, respectively. By considering that the nickel-based TMFE is the best, a $\Delta\phi$ value of about 0.2 eV is considered to be most suitable for an ideal TMFE. In this connection, the cobalt-based TMFE (the work function of cobalt equals 4.7 eV,¹⁹⁾ $\Delta\phi=0.2$ eV) was stable and showed a large H-overpotential; *i.e.*, E_p^\dagger was -1.38 V at the mercury ($120 \mu\text{g cm}^{-2}$)-coated cobalt electrode, and E_p^\dagger did not change upon standing for 70 h.

In the present work, the hydrogen-evolution reaction at the electrode surface was employed in order to investigate the electrode property because of its simplicity and reproducibility of the measurements, though other electrochemical measurements such as pzc, which may be closely correlated to the work function of the electrode surface, can be employed for this purpose.

The T-Hg curve is considered to be most available and the simplest for studying the structure of the deposited mercury film directly.

Application of Nickel-based TMFE

The nickel-based TMFE recommended in this work was applied to the anodic stripping voltammetric (ASV) determinations of copper(II), bismuth(III), lead(II), thallium(I), and cadmium(II) in an electrolyte which consisted of 0.5 M of ammonium acetate and 0.1 M of tartaric acid, and the results were compared with the results obtained using the platinum-based TMFE and the HMDE. The mercury layer of the TMFE was $200 \mu\text{g cm}^{-2}$ (ca. $0.15 \mu\text{m}$ thick). After electrolysis at -0.90 V for 2 min in a stirred solution containing $1 \times 10^{-7} \text{ M}$ of metal ions, the voltammogram was recorded anodically from -0.90 to 0 V at a rate of 50 mV s^{-1} .

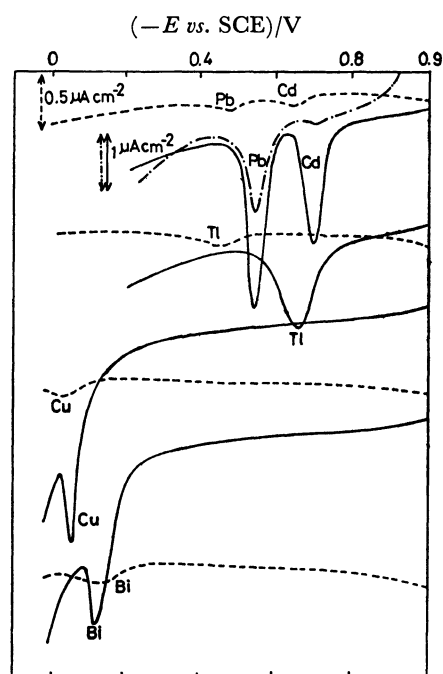


Fig. 7. ASV curves of copper (II), bismuth (III), lead (II), thallium (I), and cadmium (II) using nickel- or platinum-based TMFE and HMDE.

Electrodes; — mercury ($200 \mu\text{g cm}^{-2}$)-coated nickel, --- mercury ($200 \mu\text{g cm}^{-2}$)-coated platinum, HMDE. Electrolyte solution; 0.5 M ammonium acetate and 0.1 M tartaric acid containing $1 \times 10^{-7} \text{ M}$ of metal ions. Pre-electrolysis; at -0.9 V for 2 min with stirring. ASV; from -0.9 to 0 V at a rate of 50 mV s^{-1} .

As is shown in Fig. 7, the ASV curves obtained by the use of the nickel-based TMFE are more quantitative than those obtained using the HMDE.

When lead and cadmium were simultaneously determined using the nickel-based TMFE, the peak heights in ASV were nearly proportional to the concentrations of the metal ions of 5×10^{-9} — $2 \times 10^{-7} \text{ M}$. The standard deviations for the determinations of $5 \times 10^{-9} \text{ M}$ of lead and cadmium obtained from five repeated runs

were within 5%. The TMFE which had been left standing for 5 d after preparation gave reproducible ASV curves.

When the platinum-based TMFE was used instead of the nickel-based TMFE, the peak height in ASV for lead was proportional to the concentration of lead(II) of 2×10^{-8} — $2 \times 10^{-7} \text{ M}$, and $2 \times 10^{-8} \text{ M}$ of lead(II) was determined with a standard deviation of about 10%. No ASV peak of cadmium was obtained when the concentration was less than $1 \times 10^{-7} \text{ M}$. The platinum-based TMFE was unstable and could not be used in the ASV determination of cadmium, because hydrogen evolution at the electrode started at about -0.65 V and E_p was at -0.8 V when the electrode had been left standing for 5 h after preparation.

Thus, the nickel-based TMFE is superior to the HMDE and the platinum-based TMFE which have usually been used for the determination of trace metal ions by ASV.

The author would like to thank Dr. Sorin Kihara, Professor Taichiro Fujinaga and his coworkers, and Dr. Kenji Motoiima for their helpful discussions and useful suggestions.

References

- 1) A. M. Hartley, A. G. Hiebert, and J. A. Cox *J. Electroanal. Chem.*, **17**, 81 (1968).
- 2) K. Z. Brainina, *Talanta*, **18**, 513 (1971).
- 3) G. E. Bartley and T. M. Florence, *J. Electroanal. Chem.*, **55**, 23 (1974).
- 4) Z. Stojek and Z. Kublik, *J. Electroanal. Chem.*, **60**, 349 (1975).
- 5) T. M. Florence and G. E. Bartley, *J. Electroanal. Chem.*, **75**, 791 (1977).
- 6) L. Sipos, S. Kozar, I. Kontusic, and M. Branica, *J. Electroanal. Chem.*, **87**, 347 (1978).
- 7) Z. Yoshida, *Bull. Chem. Soc. Jpn.*, **54**, 556 (1981).
- 8) N. Furuya and S. Motoo, *J. Electroanal. Chem.*, **88**, 151 (1978).
- 9) N. Furuya and S. Motoo, *Denki Kagaku*, **41**, 364 (1973).
- 10) N. Furuya and S. Motoo, *J. Electroanal. Chem.*, **72**, 165 (1976).
- 11) N. Furuya and S. Motoo, *Denki Kagaku*, **41**, 307 (1973).
- 12) P. B. Hirsch, A. Howie, P. B. Nicholson, D. M. Pashley, and M. J. Whelan, "Electron Microscopy of Thin Crystals," Butterworths, London (1965), p. 455.
- 13) Z. Yoshida and S. Kihara, *J. Electroanal. Chem.*, **86**, 167 (1978).
- 14) M. Hansen and K. Anderko, "Constitution of Binary Alloys," McGraw-Hill, New York (1958).
- 15) Z. Yoshida and S. Kihara, *J. Electroanal. Chem.*, **95**, 159 (1979).
- 16) D. M. Kolb, "Advances in Electrochemistry and Electrochemical Engineering," Wiley-Interscience, New York (1978), Vol. 11, p. 125.
- 17) D. M. Kolb, M. Przasnyski, and H. Gerischer, *J. Electroanal. Chem.*, **54**, 25 (1974).
- 18) M. Z. Hassan, D. F. Untereker, and S. Bruckenstein, *J. Electroanal. Chem.*, **42**, 161 (1973).
- 19) S. Trasatti, *J. Electroanal. Chem.*, **33**, 351 (1971).
- 20) S. Trasatti, *J. Electroanal. Chem.*, **54**, 19 (1974).
- 21) S. Trasatti, *J. Electroanal. Chem.*, **39**, 163 (1972).